Journal of Physics: Conference Series **527** (2014) 012014 doi:10.1088/1742-6596/527/1/012014

Equations of state based on recent lattice QCD results at vanishing net-baryon density

P Alba[1], W Alberico[1], A Beraudo[2], M Bluhm[3], C Ratti[1]

[1] Dipartimento di Fisica, Università degli Studi di Torino & INFN, Sezione di Torino, via Giuria 1, I-10125 Torino, Italy
[2] Physics Department, Theory Unit, CERN, CH-1211 Genève 23, Switzerland
[3] Department of Physics, North Carolina State University, Raleigh, NC 27695, USA

E-mail: pgalba@to.infn.it

Abstract. We calculate various equations of state for QCD matter at vanishing net-baryon density starting from recent lattice QCD results at high temperatures, going to low temperatures using a hadron resonance gas (HRG) model to describe the confined phase. In order to have a better description of the experimental situation we use an implementation of the HRG model that allows the system to switch, after the chemical freeze-out, to a situation of partial chemical equilibrium. We explore the possibility of different freeze-out temperatures. Our results can be used in the hydrodynamic modeling of relativistic heavy-ion collisions at the LHC and at the highest RHIC beam energies.

1. Introduction

In relativistic heavy-ion collision experiments currently taking place at RHIC (Relativistic Heavy-Ion Collider) and at the LHC (Large Hadron Collider), the deconfined phase of strongly interacting matter, called Quark-Gluon Plasma (QGP), is transiently created. The QGP is formed immediately after the collision; the system then cools down and expands and matter goes through a phase transition from the QGP into a confined hadron gas. The transition is an analytic crossover, as unambiguously proven by first-principle simulations of QCD on the lattice [1]. The transition takes place at a pseudo-critical temperature T_c which has recently been estimated in lattice QCD simulations as well [2, 3].

Relativistic hydrodynamics (see e.g. the reviews in Refs. [4, 5]) has been very successful in modelling the collective dynamics of the matter created in the laboratory, starting from a stage immediately after thermalization until the kinetic freeze-out of final state hadrons. The evolution of the system is driven by the conservation equations for energy, momentum and for the additionally conserved charges (net-baryon number N_B, net-electric charge N_Q and net-strangeness N_S), under the assumption of local thermal equilibrium. The Equation of State (EoS) is an essential ingredient for hydrodynamic simulations: it provides a relation between energy density ϵ, pressure p and the densities n_B, n_Q and n_S of the conserved charges. Assuming the conservation of entropy, one needs to know the EoS only along adiabatic paths. In particular we will follow the path $n_B/s = 0$, i.e. we consider the situation of a vanishing n_B. In addition, to get closer to the situation realized in a heavy-ion collision, we impose $n_S = 0$, while the relationship between n_Q and n_B is fixed by the Z/A of the colliding nuclei.

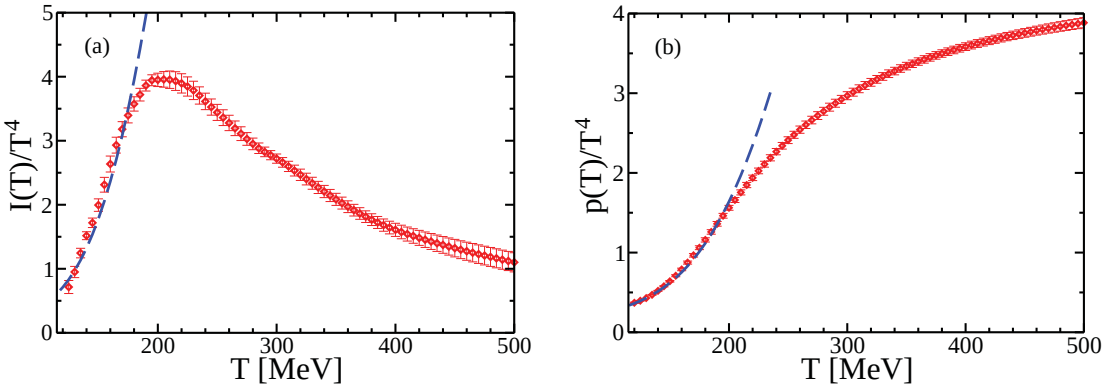

Figure 1. (Color online) Scaled interaction measure $I(T)/T^4$ (panel (a)) and pressure $p(T)/T^4$ (panel (b)) as functions of the temperature T. The symbols correspond to the lattice QCD results from [10]; the dashed curves are the results of the HRG model in thermodynamic equilibrium.

Lattice gauge theory simulations for the QCD equation of state reach nowadays unprecedented levels of accuracy. A basic quantity for the EoS is the interaction measure $I = \epsilon - 3p$, which has been calculated in [6, 7] and in [8, 9, 10]. The numerical results for $I(T)/T^4$ in [6, 7] show significant differences from those in [9, 10] in the transition region. We opt for utilizing in our work the most recent, continuum-extrapolated lattice QCD data from the WB-collaboration [10], corresponding to a system of 2+1 quark flavors with physical quark masses.

We build up a baseline QCD equation of state for $n_B = 0$, by combining a suitable parametrization of these lattice QCD results with a hadron resonance gas (HRG) model in thermodynamic equilibrium. We implement partial chemical equilibrium (i.e. a non-equilibrium situation) in the hadronic phase, in order to properly account for the actual chemical composition in the confined phase. This issue cannot be addressed within equilibrium lattice QCD thermodynamics, but it is of fundamental importance in order to reproduce the experimentally observed flow and p_T-spectra, as well as the correct particle ratios [11]. Because of the present uncertainty in its exact value [12, 13], we study various values for the chemical freeze-out temperature T_{ch}, below which the HRG is in partial chemical equilibrium. Having such QCD equations of state at hand will allow a more controlled determination of the QGP transport properties, as for example the shear (and bulk) viscosity coefficients, and even more important to check which modification to the thermodynamics would imply a variation of 15 MeV in T_{ch}.

This proceeding contribution is organized as follows: in section 2, we show how to combine the lattice QCD results with an HRG model in thermodynamic equilibrium. Section 3 deals with the inclusion of partial chemical equilibrium in the hadronic phase. In section 4, we discuss the obtained QCD equations of state and discuss their main features. For more details we refer the reader to Ref. [14].

2. Lattice QCD-based EoS

Continuum-extrapolated lattice QCD results for thermodynamic quantities in a system of 2+1 quark flavors with physical quark masses were presented in [10]. Their results for the scaled interaction measure $I(T)/T^4$ and for the scaled pressure $p(T)/T^4$ are shown in figure 1 panels (a) and (b), respectively. The other thermodynamic quantities can be obtained from $I(T)$ and $p(T)$ via $\epsilon(T) = 3p(T) + I(T)$ and $s(T) = (\epsilon(T) + p(T))/T$.

QCD thermodynamics in the hadronic phase can be understood in terms of the HRG model,

which describes hadronic matter in thermodynamic equilibrium, see e.g. Refs. [15, 16]. The pressure of the model in the thermodynamic limit is given by

$$p(T,\{\mu_k\}) = \sum_k (-1)^{B_k+1} \frac{d_k T}{(2\pi)^3} \int d^3\vec{p}\ \ln\left[1 + (-1)^{B_k+1} e^{-(\sqrt{\vec{p}^2+m_k^2}-\mu_k)/T}\right], \quad (1)$$

where the sum is taken over all the hadronic (including resonances) states k included in the model. In equation (1), d_k and m_k are the degeneracy factor and the mass, and μ_k is the chemical potential of the hadron-species k. In chemical equilibrium, the latter reads $\mu_k = B_k\mu_B + Q_k\mu_Q + S_k\mu_S$, where B_k, Q_k and S_k are the respective quantum numbers of baryon charge, electric charge and strangeness, while μ_B, μ_Q and μ_S denote the chemical potentials associated with n_B, n_Q and n_S.

The particle number density of species k, $n_k = (\partial p/\partial\mu_k)_T$, is given by

$$n_k(T,\mu_k) = \frac{d_k}{(2\pi)^3} \int d^3\vec{p} \frac{1}{(-1)^{B_k+1} + e^{(\sqrt{\vec{p}^2+m_k^2}-\mu_k)/T}} \quad (2)$$

and the net-baryon density follows from $n_B = \sum_k B_k n_k$. Since the vanishing n_B is considered, all μ_k are set to zero in the chemical equilibrium case.

The HRG model used in this work contains states with mass up to 2 GeV as listed in the edition [17] of the Particle Data Book, as well as in the EoS-package provided in [18].

We construct an equation of state which serves as a baseline for the chemical equilibrium case by using our suitable parametrization of the lattice QCD results from [10] at high T and switching to the HRG model at low T around a temperature of 172 MeV. In order to avoid discontinuities in the thermodynamic quantities, which can generally arise in such an approach, we employ a straightforward interpolation procedure between the two parts in the interval 165 MeV $\leq T \leq$ 180 MeV. Such a procedure ensures that the pressure and its first and second derivatives with respect to T are continuous functions, like for example the speed of sound which shows a smooth behavior for all the temperatures in the considered range.

3. Hadron resonance gas in partial chemical equilibrium

A realistic description of a heavy ion collision assumes that the hadronic phase is not in complete chemical equilibrium, since the time scales for inelastic particle number changing processes are typically much larger than the lifetime of the hadronic stage [19]. This was first discussed in [20] and then considered in numerous works, see e.g. Refs. [11, 21, 22, 23, 24]. At the hadronization temperature T_c, hadronic matter is formed in chemical equilibrium; subsequently for temperatures below the chemical freeze-out temperature T_{ch} (with $T_{ch} \leq T_c$) the inelastic processes become suppressed, while the elastic interactions mediated by frequent strong resonance formation and decays (e.g. $\pi\pi \to \rho \to \pi\pi$, $K\pi \to K^* \to K\pi$, $p\pi \to \Delta \to p\pi$ etc.) continue to occur. As a consequence, the experimentally observed ratios of particle multiplicities of those species i, which are stable against strong decays within the lifetime of the system, are fixed at T_{ch}. Namely, for $T < T_{ch}$ their effective particle numbers $\bar{N}_i = N_i + \sum_r d_{r\to i} N_r$ are frozen, where N_i is the particle number of the stable hadron i, N_r the particle number of resonance r and $d_{r\to i}$ gives the average number of hadrons i produced in the decay of resonance r. The above sum is taken over all the resonances that decay into hadron i within the lifetime of the hadronic stage. Each stable particle species i acquires therefore an effective chemical potential $\mu_i(T)$. The chemical potentials of the resonances can the be written as a combination $\mu_r = \sum_i d_{r\to i}\,\mu_i$ of the ones of the stable particles.

The EoS is obtained as a highly-involved relation between p, ϵ and all charge densities: this is due to the conservation of the effective number $\bar{N}_i$ of each stable particle species i below T_{ch}.

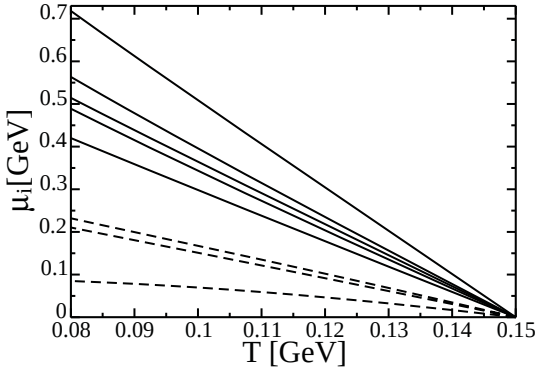

Figure 2. Temperature-dependence of the effective chemical potentials for selected hadronic states, for a chemical freeze-out temperature of $T_{ch} = 150$ MeV. The solid curves depict $\mu_i(T)$ for the baryons Ω^-, Ξ^-, Σ^-, Λ^0 and p from top to bottom, while the dashed curves show $\mu_i(T)$ for the mesons η, K^- and π^+ from top to bottom.

Assuming the conservation of entropy, the ratio between the effective particle number density and the entropy density $\bar{n}_i/s$ is fixed at T_{ch}. The following conditions, which imply that each $\bar{n}_i$ depends on all the effective chemical potentials $\mu_{i'}(T)$ (including $\mu_i(T)$), provide a practical tool to conserve all the $\bar{N}_i$ and to determine all the $\mu_i(T)$ for $T < T_{ch}$:

$$\frac{\bar{n}_i(T, \{\mu_{i'}(T)\})}{s(T, \{\mu_{i'}(T)\})} = \frac{\bar{n}_i(T_{ch}, \{0\})}{s(T_{ch}, \{0\})}. \tag{3}$$

Besides being needed for the determination of the EoS, the knowledge of all the $\mu_i(T)$ is necessary to determine the final state hadron abundances.

In this work, we consider as stable particle species the mesons π^0, π^+, π^-, K^+, K^-, K^0, $\overline{K}^0$ and η and the baryons p, n, Λ^0, Σ^+, Σ^0, Σ^-, Ξ^0, Ξ^- and Ω^- as well as their respective anti-baryons, i.e. in total 26 different states. For the chemical freeze-out temperature, we consider different values, namely T_{ch}/MeV= 145, 150, 155 and 160. These are within the range of the T_c-values determined in lattice QCD [2, 3].

In figure 2, we show the behavior of the effective chemical potentials $\mu_i(T)$ as functions of the temperature, for some exemplary particle species in the case $T_{ch} = 150$ MeV. The $\mu_i(T)$ increase with decreasing T, as one would expect since the stable states become more populated by resonance decays at low temperatures. In the related published paper [14] we provide a parametrization of such chemical potentials, with a table of the parameters needed to obtain them.

4. Discussion and Conclusions

We obtained various equations of state by continuously combining our parametrization of the lattice QCD data [10] as a function of T with the HRG model either in full or in partial chemical equilibrium in the hadronic phase. The latter case has been studied for various T_{ch}-values. In hydrodynamic simulations, however, the EoS is used in the form $p(\epsilon, n_B)$, i.e. as a function of ϵ and n_B, as well as the results for the effective chemical potentials μ_i are required for the determination of the particle abundances. In figure 3, we show our results for the different equations of state $p(\epsilon)$ supplemented by the corresponding $T(\epsilon)$ for $n_B = 0$. In figure 3 we focus on the energy density regions, in which the confinement transition and the chemical freeze-out take place.

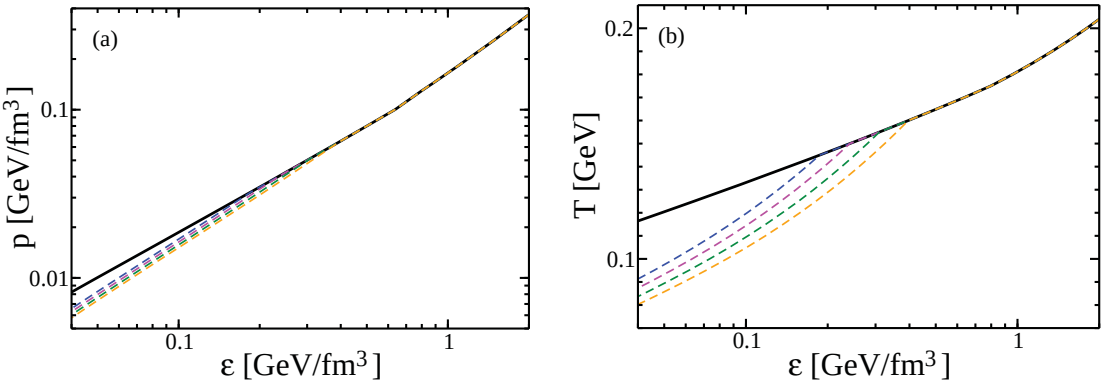

Figure 3. (Color online) (a) Equations of state $p(\epsilon)$ for $n_B = 0$ zoomed into the regions in ϵ, in which the confinement transition and the chemical freeze-out occur. The solid curve corresponds to the HRG model in chemical equilibrium. For the dashed curves, partial chemical equilibrium is included below ϵ_{ch}. The value of ϵ_{ch} depends on the value of the freeze-out temperature T_{ch}. We consider $T_{ch}/\mathrm{MeV} = 145$, 150, 155 and 160 (from top to bottom in the figure, respectively). (b) Temperature vs. energy density $T(\epsilon)$ for the equations of state with chemical equilibrium (solid curve) and with partial chemical equilibrium (dashed curves) (labelling as in panel (a)).

The differences in $p(\epsilon)$ between chemical equilibrium (solid curve) and partial chemical equilibrium (dashed curves) in the hadronic phase turn out to be small, while the ϵ-dependence of T is significantly influenced, for $\epsilon < \epsilon_{ch}$, by the chemical freeze-out (see panel (b) in figure 3). Our results are collected in tabulated form and made available in [25]. For practical convenience, in [14] we also provide parameterizations of these numerical results as functions of ϵ.

The high precision in the provided parameterization is motivated by our goal to maintain thermodynamic consistency and continuity in the second derivatives up to a high numerical accuracy.

The temperature-dependence of the speed of sound c_s^2 obtained by numerical differentiation, is shown in figure 4 (solid curve) and compared to the lattice QCD results available from the WB-collaboration [9]. In the case of full chemical equilibrium, our curve agrees with the lattice QCD data within error-bars: in particular, we find a rather large $c_s^2(T)$ in the confinement transition region. This indicates that our EoS is rather stiff. The dashed curves correspond to the partial chemical equilibrium case. One observes a discontinuity in $c_s^2(T)$ at $T = T_{ch}$, which is characteristic for the chemical freeze-out. As expected, the behavior of $c_s^2(T)$ in the non-equilibrium situation is different from the trend seen in equilibrium lattice QCD thermodynamics.

In summary, we constructed QCD equations of state for vanishing net-baryon density based on recent continuum-extrapolated lattice QCD results in the physical quark mass limit at high T [10], continuously combined with a HRG model at low T. The latter was considered to be either in chemical or in partial chemical equilibrium. Focusing on the partial chemical equilibrium case, we studied different values for the chemical freeze-out temperature within its presently expected range [12].

In the present work, we focused ourselves to the $n_B = 0$ case. Therefore, our results can be used as an input in the hydrodynamic modeling of high-energy heavy-ion collisions at the LHC and at RHIC top beam energies and at mid-rapidity. We will address the equation of state in partial chemical equilibrium at finite density in a forthcoming publication.

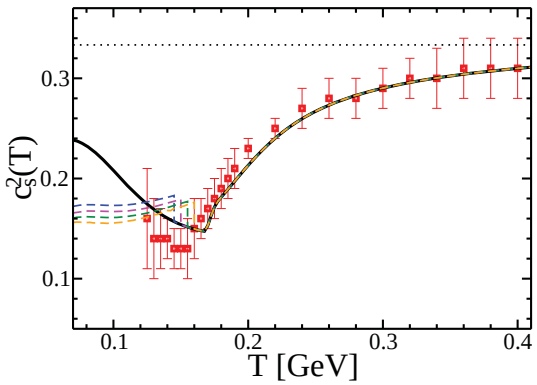

Figure 4. (Color online) Temperature-dependence of the squared speed of sound $c_s^2(T)$. The solid curve corresponds to the HRG model in chemical equilibrium. The symbols represent available equilibrium lattice QCD data from [9]. The dashed curves highlight $c_s^2(T)$ when partial chemical equilibrium is assumed in the hadronic phase. We consider $T_{ch}/\mathrm{MeV} = 145$, 150, 155 and 160 (from top to bottom, respectively).

References

[1] Aoki Y, Endrodi G, Fodor Z, Katz S D, and Szabo K K 2006 *Nature* **443** 675
[2] Borsanyi S *et al.* 2010 *J. High Energy Phys.* **1009** 073
[3] Bazavov A *et al.* 2012 *Phys. Rev. D* **85** 054503
[4] Kolb P F and Heinz U in *Quark Gluon Plasma 3*, edited by Hwa R C and Wang X N 2004 *World Scientific, Singapore* p. 634
[5] Gale C, Jeon S, and Schenke B 2013 *Int. J. of Mod. Phys. A* **28** 1340011
[6] Bazavov A *et al.* 2009 *Phys. Rev. D* **80** 014504
[7] Cheng M *et al.* 2010 *Phys. Rev. D* **81** 054504
[8] Aoki Y, Fodor Z, Katz S D, and Szabo K K 2006 *J. High Energy Phys.* **0601** 089
[9] Borsanyi S *et al.* 2010 *J. High Energy Phys.* **1011** 077
[10] Borsanyi S *et al.* 2011 *Proc. of Sci.* **LATTICE2011** 201
[11] Hirano T and Tsuda K 2002 *Phys. Rev. C* **66** 054905
[12] Borsanyi S, Fodor Z, Katz S D, Krieg S, Ratti C, and Szabo K K 2013 *Phys. Rev. Lett.* **111** 062005
[13] Borsanyi S, Fodor Z, Katz S D, Krieg S, Ratti C, and Szabo K K 2014 `arXiv:1403.4576`
[14] Bluhm M *et al.* 2013 `arXiv:1306.6188`
[15] Karsch F, Redlich K, and Tawfik A 2003 *Phys. Lett. B* **571** 67
[16] Tawfik A 2005 *Phys. Rev. D* **71** 054502
[17] Eidelman S *et al.* [Particle Data Group] 2004 *Phys. Lett. B* **592** 1
[18] Huovinen P and Petreczky P 2010 *Nuc. Phys. A* **837** 26
[19] Teaney D 2002 `arXiv:nucl-th/0204023`
[20] Bebie H, Gerber P, Goity J L, and Leutwyler H 1992 *Nuc. Phys. B* **378** 95
[21] Rapp R 2002 *Phys. Rev. C* **66** 017901
[22] Kolb P F and Rapp R 2003 *Phys. Rev. C* **67** 044903
[23] Huovinen P 2008 *Eur. Phys. J. A* **37** 121
[24] Del Zanna L *et al.* 2013 `arXiv:1305.7052`
[25] `http://personalpages.to.infn.it/~ratti/EoS/Equation_of_State/Home.html`